Effect of room-temperature out-time on tow impregnation in an out-of-autoclave prepreg

L.K. Grunenfelder[1*], T. Centea[2], P. Hubert[2], S.R. Nutt[1]

1. Department of Chemical Engineering and Materials Science, University of Southern California, Los Angeles, CA 90089-0241, USA
2. Department of Mechanical Engineering, McGill University, Montreal, Quebec, Canada H3A 2A7

*Corresponding author: grunenfe@usc.edu

Abstract: Tow impregnation as a function of material out-time was investigated for an out-of-autoclave carbon fiber–epoxy prepreg. Prepreg was aged at ambient temperature for 56 days. Every 7 days, laminates were laid up and cured using vacuum bag only processing. Void content was calculated through image analysis of polished sections. Experimental results were used to validate an analytical model for tow impregnation. Model predictions were based on flow kinetics during processing conditions, taking into account increasing degree of cure and evolution of resin viscosity as a function of ambient aging time. The study found that no significant tow porosity occurred within the material's stated out-life, that tow porosity increased once this out-life was exceeded and eventually stabilized due to the room-temperature vitrification of the resin. The model's predicted trends were consistent with experimental results, suggesting that an increase in resin viscosity is indeed the main cause of out-time induced tow porosity and providing a means of predicting laminate quality as a function of room temperature aging time.

Key words: A. Laminates; A. Prepreg; B. Porosity; C. Analytical modeling

1. Introduction

The use of composite parts in the aircraft industry has increased steadily in recent decades [1]. The demand for air travel is also increasing, resulting in the need for a cost-effective and efficient means

L.K. Grunenfelder, T. Centea, P. Hubert, S.R. Nutt, **"Effect of room-temperature out-time on tow impregnation in an out-of-autoclave prepregs,"** Composites Part A: Applied Science and Manufacturing, 45, 119-126 (2012), DOI: **http://dx.doi.org/10.1016/j.compositesa.2012.10.001**

of manufacturing large composite structures. Presently, most composite parts for high-performance aerospace applications are manufactured using autoclaves. During autoclave processing, high temperatures and pressures are applied to consolidate and cure composite structures. However, there are multiple drawbacks to autoclave processing, including high capital and operational costs, poor energy efficiency, long cycle times, and part size constraints [2] and [3]. To address these issues, manufacturers have introduced a new generation of out-of-autoclave prepregs designed for oven-curing under vacuum [2] and [3]. These vacuum bag-only (VBO) out-of-autoclave (OOA) prepregs consist of carbon fibers pre-impregnated with epoxy resin. VBO prepregs offer clear advantages over conventional prepregs, but before they can be used in aerospace applications, the mechanisms of void formation in low-pressure processing must be better understood.

VBO prepregs are designed to suppress void formation through a method of partial resin impregnation. By design, VBO prepregs initially contain a connected network of dry, unimpregnated regions, referred to as engineered vacuum channels (EVaCs), sandwiched between resin films [4], [5], [6], [7], [8] and [9]. Upon application of vacuum, air within the prepreg can escape through these channels towards the edges, where it is removed via edge-breathing consumables [10]. Similarly, air may also travel in the through-thickness direction of the laminate, and escape through the surface. The transverse permeability of a laminate depends on macro- and micro-characteristics of the prepreg, including the EVaCs [11]. After air and volatiles are removed, the EVaCs must be fully impregnated by resin flow to achieve a void-free part. The introduction of partially impregnated VBO prepregs has allowed for the production of high-quality parts with vacuum pressure only [1] and [5]. Removing the requirement for autoclave pressures eliminates the size constraints associated with autoclave cure and allows for the manufacture of large integrated structures at lower cost [2], [5] and [12].

While the manufacture of large parts with out-of-autoclave methods is appealing, the long times required to lay up large structures may exceed the out-time limits, or time allowed at room temperature, of present VBO prepreg systems. The "out time" or "aging" allowed for prepregs derives from the fact that epoxy resins are unstable at ambient temperature, and must be stored frozen until used [13], [14], [15] and [16]. The lay-up of large parts, however, requires long preparation times, during which the material is exposed to ambient conditions [12], [14], [15] and [16]. Studies have shown that epoxy resins in prepregs undergo chemical changes during ambient aging, which can adversely affect both processability and final part quality [14], [15], [17], [18] and [19]. While the chemical aging of epoxy-based prepregs has been studied extensively, few studies have examined the influence of resin aging on the properties of cured laminates [18].

Past reports on mechanical properties of composites as a function of aging before processing have yielded conflicting results [14]. Short beam shear strength, or interlaminar shear strength (ILSS), a matrix driven property, is often examined in out-time studies. Some material systems show little or no change in ILSS as a function of out-time [13] and [14], while other systems display a decrease in ILSS with out-time [16], [17] and [19]. While mechanical property measurements provide an indication of part quality, the critical parameter influencing part acceptance for carbon fiber structures is porosity. Understanding the processes by which porosity is removed (or not) is particularly critical when adopting low-pressure processes, where the safeguards to void formation provided by high compaction pressures are absent. In this work, we present experimental data and analysis of void content in VBO-processed laminates as a function of ambient out-time in an effort to determine the latter's effects on air removal and porosity.

For VBO prepregs to gain acceptance in industry, improved understanding of the sources of voids and the evolution of microstructure is required. There are examples in the literature of experimental work showing reduced compaction and increased porosity in VBO-processed parts [12] and [16], as well as analytical work that has predicted incomplete infiltration [20], particularly when the resin viscosity increases due to out-time [21]. However, neither experimental measurements alone nor analytical models (without validation) provide insights sufficient to understand void formation and control porosity, and an integrated experimental/analytical investigation is necessary.

Here, we present an approach to the understanding of impregnation in OOA prepregs that integrates both experiments and modeling. First, the presence of tow voids in aged laminates is investigated experimentally through the manufacture of test panels exposed to various ambient aging times. We adapt an analytical model for tow impregnation in the selected VBO prepregs, and employ the model to predict the occurrence of tow voids in laminates produced from aged prepregs. Experimental observations and data are used to validate the model predictions, and comparisons are analyzed. The complementary experimental and analytical components provide insights and understanding of the material aging and tow impregnation processes, as well as a means to predict part quality as a function of prepreg aging time.

2. Experiments

2.1 Material

The material selected for this study was a carbon fiber–epoxy prepreg formulated for vacuum-bag-only cure. The prepreg was composed of a 5-harness–satin (5HS) carbon fiber fabric and a toughened

epoxy resin (CYCOM 5320, Cytec Engineered Materials, USA). The manufacturer's stated out-life for the material system was 3 weeks at ambient temperature.

2.2 Prepreg initial condition

Imaging of the studied material in the as-received condition was performed to determine the geometry of engineered vacuum channels. The microstructure of the prepreg prior to processing was first analyzed using X-ray microtomography, or micro-CT, according to the procedure described in [6]. A laminate measuring approximately 100 × 150 mm and consisting of four layers of 5HS prepreg was laid up at room temperature. A sample approximately 15 × 15 mm was sectioned from the laminate and scanned using a high-resolution X-ray microtomograph (Skyscan 1172). The scan parameters consisted of a 4000 × 2096 pixel image, 6.9 μm/pixel, a source voltage and current of 64 kV and 157 μA, and an exposure time of 1178 ms. No filter was used. The scanned data was reconstructed into a series of parallel micro-slices, providing two- and three-dimensional information about the porosity distribution within the material.

Additionally, a single ply of prepreg was imaged by scanning electron microscopy (JEOL JSM-6610-SEM). To prepare the material for SEM imaging, a single ply was cured at room temperature for several weeks. After room temperature cure, resin had solidified to the point that a low-speed diamond blade could be used to section the prepreg. The resin was never heated, thereby precluding resin flow and preserving the original distribution of resin within the fabric.

Fig. 1a shows a stack of unprocessed prepreg plies imaged using micro-CT, and an SEM image of a single ply is presented in Fig. 1b. The partial impregnation of plies and the presence of dry fiber channels (EVaCs) in the prepreg is clear in these images. This visual inspection of unconsolidated

prepreg plies provides necessary documentation of the structure of the material and the initial level of resin impregnation.

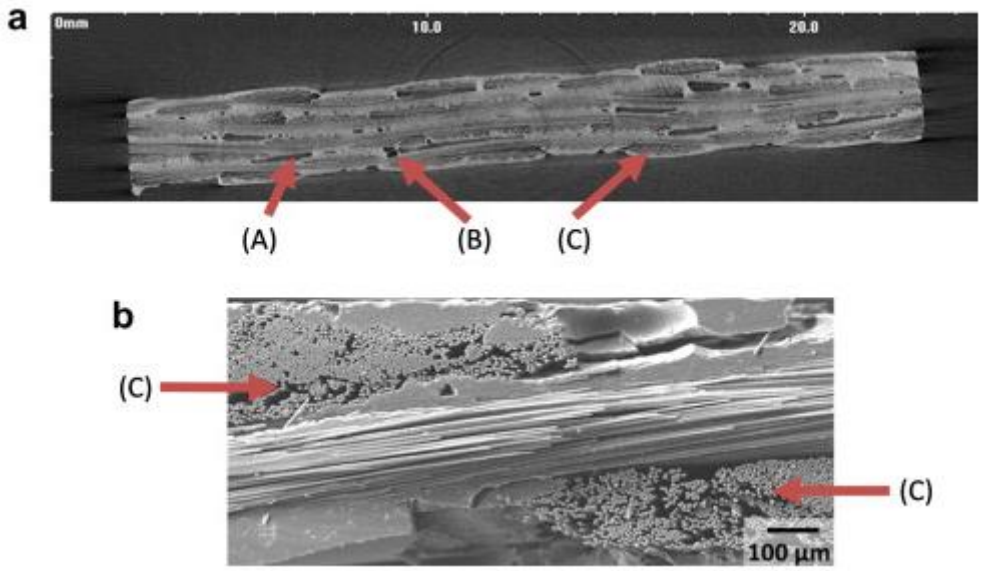

Figure 1: *(a) Micro-CT image showing the initial condition in a stack of prepreg plies, (b) SEM image of a single prepreg ply in the as-received condition. Void types are labeled with letters, (A) inter-laminar voids, (B) inter-tow gaps, and (C) fiber tow voids. (For interpretation of the references to color in this figure legend, the reader is referred to the web version of this article.)*

The prepreg in the initial condition contains a large percentage of void volume. Examination of the micro-CT image in Fig. 1a shows distinct void types [4] and [6]. The large planar voids in the regions between plies are inter-laminar voids (A) caused by air entrapped in gaps during the lay-up process. Large quasi–spherical voids are present within a given ply, in the resin-rich areas making up the inter-tow gaps (B). Small void areas are present within the fiber tows (C), visible as dark elliptical shapes. Based on a volumetric analysis method of the micro-CT data [6], the initial percent content of macro-voids (types A and B) is estimated at 8.5%. Furthermore, it may be seen from Fig. 1a that the majority of the tow cross-section is unimpregnated. For tows with fiber volume fractions of 0.6–

0.75, as typically found in VBO prepregs [21], the percent content of type C voids within the tows could thus be as high as 25–40%.

Fiber tow voids can be distinguished more clearly in Fig. 1b (arrow), which clearly shows the unimpregnated dry fiber regions at the center of the fiber tows (type C voids). These fiber tow voids are intentionally created in out-of-autoclave prepregs, to provide engineered vacuum channels (EVaCs) which allow for air removal and subsequent resin infiltration [6], [10] and [22]. In this study, the impregnation of EVaCs (fiber tow voids) was tracked as a function of material aging time. Interlaminar and inter-tow void contents were not tracked or measured.

2.3. Laminate manufacture

To produce test panels, prepreg plies were cut to dimensions of 210 × 210 mm, and aged in ambient laboratory conditions in unsealed plastic bags. Temperature and humidity in the laboratory were measured periodically during aging using a pen-style digital gauge with a traceable National Institute of Standards and Technology calibration certification (Control Company, USA). Temperature remained within the range of 20 ± 2 °C, and humidity levels of 50 ± 5% RH were recorded. 8-ply quasi-isotropic laminates [0/±45/90]s were laid up and cured every 7 days as aging progressed. Samples were bagged according to a standard vacuum bagging assembly. The lay-up configuration is presented in Fig. 2a. Bagged laminates were cured in an oven under vacuum pressure. A two-temperature dwell combined cure schedule was implemented, as dictated by the prepreg manufacturer, consisting of a 1.5 °C/min ramp to 121 °C, a 1 h hold, a 1.5 °C/min ramp to 177 °C and a 2 h hold [23]. Thermocouple measurements, from a thermocouple located at the tool surface, showing the temperature cycle during cure are presented in Fig. 2b, indicating that the laminates

underwent the recommended cure cycle. No room temperature debulk was performed, and vacuum was pulled continuously during cure.

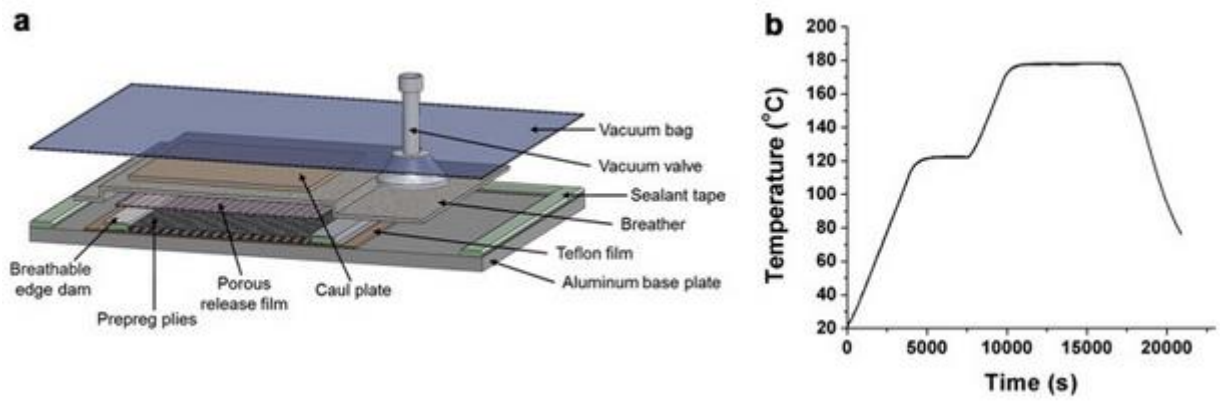

Figure 2: *(a) Vacuum bagging assembly for laminate manufacture, (b) thermocouple measurements of temperature at the tool surface (aluminum base plate) during the cure cycle. (For interpretation of the references to color in this figure legend, the reader is referred to the web version of this article.)*

2.4. Void content

Cured laminates were characterized to determine tow impregnation as a function of aging time. Samples were sectioned at the center of each panel, and three sections from each test laminate were mounted and polished. Polished sections were imaged using a digital stereo microscope (Keyence VH-Z100R). The void content within fiber tows was calculated using image analysis as the average ratio of tow void area Av to total tow area Atow of 20 tows for each sample. Void content outside the fiber tows was not tracked in this study. However, interlaminar voids were observed in panels with 0 and 7 day out-times, though void content was less than 1%. Voids between plies in fresh prepreg were assumed to arise due to high resin tack [14] and [16]. Interlaminar voids were not observed in panels aged for more than 7 days. Representative microscope images, showing tow void content for each test sample are presented in Fig. 3. Inset numbers indicate material out-time.

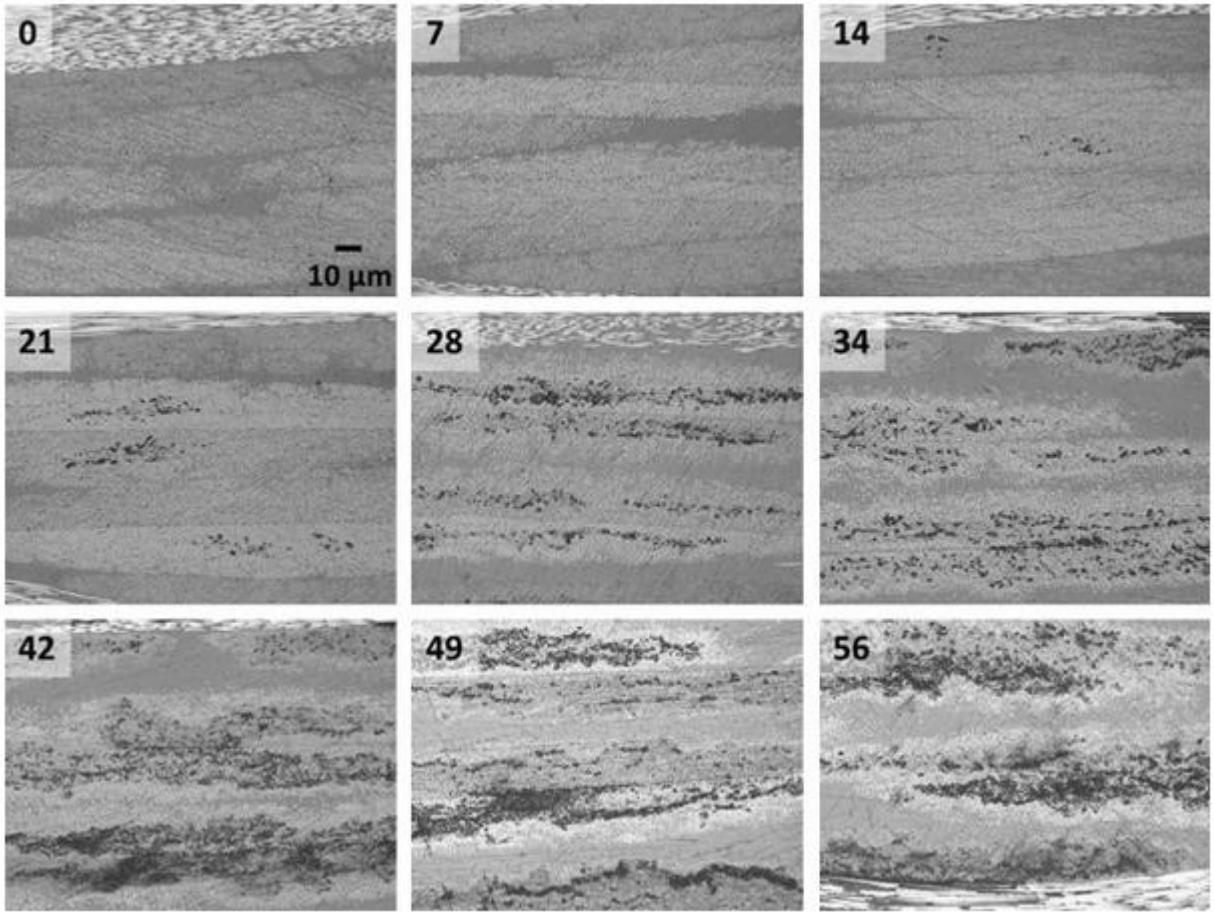

Figure 3: *Micrographs of tow impregnation in aged samples (number of days aged indicated).*

The micrographs in Fig. 3 show a decrease in laminate compaction and an increase in tow void content as a function of ambient aging time. The increase in tow porosity is a consequence of the reduction in resin viscosity that accompanies the advancement of cure during aging time [15].

Measured tow void contents are plotted as a function of prepreg out-time in Fig. 4. Note that the error bars on the experimental data points are relatively large due to variability in tow impregnation throughout the sample [6] and [24]. This variability stems from initial variations in prepreg resin impregnation, as well as the inherent variability of fiber packing and permeability within the tows. While individual tows in each sample show a range of impregnation levels, the averaging of 20 tows

provides a representative void content for the sample as a whole. The trend in the measured values shows that the tows contain negligible void content with short aging times. Between 14 and 21 days of aging, the onset of tow voids is apparent, followed by an increase in void content, and eventually a plateau in porosity level. The causes and implications of this trend are considered in the discussion section.

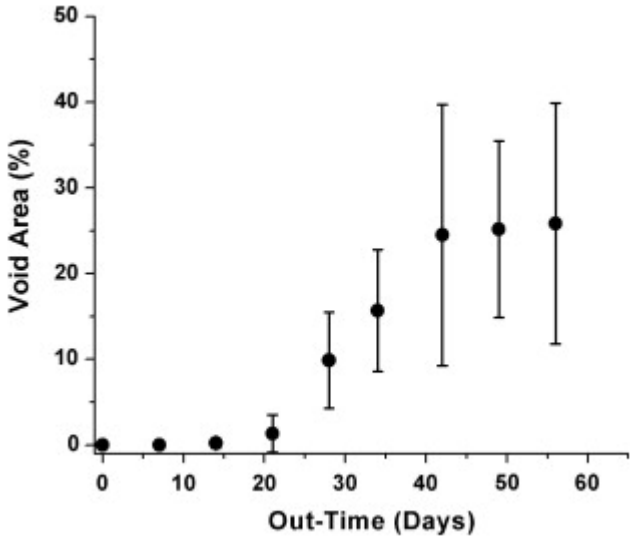

Figure 4: *Measured values of tow void content as a function of ambient aging time.*

3. Modeling

3.1. Model derivation

OOA prepregs are commonly manufactured by attaching resin films to both sides of a dry fabric. During ply collation and initial laminate compaction, these resin-rich regions thus come to be located within the macro-pore network between plies and around tows [6]. While some entrapped air may also be present within this area in the form of inter-laminar voids and inter-tow gaps, the eventual

collapse of the voids and gaps due to air evacuation and applied pressure is likely to cause local, rather than long-range, resin migration. Thus, we can assume that negligible macro-flow occurs outside the tows, and that the only dry fiber areas subject to impregnation are those within the tows.

Tow impregnation, or resin flow into dry elliptical or circular fiber bundles, has been the subject of previous modeling efforts, which generally seek to predict the flow kinetics in light of various material properties and process parameters (for example, [25], [26], [27] and [28]). In recent work, a model was described for the tow impregnation of VBO prepregs under processing conditions [21]. The model is based on Darcy's Law for the saturated flow of a viscous fluid within a rigid porous medium and mass continuity:

$$\overline{Q} = -\frac{\overline{\overline{K}} A}{\mu} \nabla P \tag{1}$$

$$\nabla \cdot \vec{v} = 0 \tag{2}$$

In Eqs. (1) and (2), View the MathML source is the flow rate of the fluid; View the MathML source is the velocity of the fluid; View the MathML source is the permeability tensor of the medium; A is the flow front area; μ is the dynamic viscosity of the fluid; and P is the pressure within the fluid. The above framework was simplified by assuming circular tows of fiber volume fraction Vf and infiltration that is axisymmetric within the cross-section and uniform along the tow length. The elliptical shape of the actual tows is taken into account when defining the value of the circular tow radius. With the radius of the resin infiltration front being Rf, the radius of the tow being Rtow and

the corresponding resin pressure boundary conditions being Pf and P∞, respectively, Eqs. (1) and (2) were combined to obtain the following expression for the resin flow front velocity:

$$v_f = \frac{dR_f}{dt} = -\frac{K}{\mu(1-V_f)}\left(\frac{1}{R_f}\frac{(P_f - P_\infty)}{\ln(R_f/R_{tow})}\right) \quad (3)$$

The model was further simplified by defining a degree of impregnation β (which increases from 0 to 1 with progressive impregnation) and normalizing Eq. (3):

$$\beta = 1 - \frac{R_f}{R_{tow}} = 1 - \sqrt{\frac{A_f}{A_{tow}}} \quad (4)$$

$$\frac{d\beta}{dt} = \frac{K}{\mu R_2^{tow}(1-V_f)}\left(\frac{(P_\infty - P_f)}{(1-\beta)\ln(1/(1-\beta))}\right) \quad (5)$$

Eq. (5) assumes that parameters K, μ, Rtow, Vf, P∞ and Pf remain constant. However, during cure, the viscosity varies due to the cure temperature and degree of polymerization. To account for this variation, the equation is solved over discrete time steps. The viscosity is assumed constant within a time step, and updated between them.

3.2. Model parameter determination

Eq. (5) can be used to predict the evolution of the degree of fiber tow impregnation for the prepreg and time–temperature cycle presented in the experimental section if the following parameters are determined: the tow volume fraction and geometry; the pressure boundary conditions P∞ and Pf; the evolution of the resin viscosity μ, and the tow transverse permeability, K. A detailed procedure for

determining these parameters is described in Ref. [21], and was applied to the current prepreg, as described below.

The tow microstructure was determined by compressing square laminate samples (layup of [0°/90°]2s, 55 ± 1 mm per side) to pre-determined thicknesses in an electromechanical test fixture (MTS Insight) with heated platens (99 ± 5 °C) and holding them at these thicknesses until vitrification. During the 0.05 mm/min compression and pre-gelation stages of the constant-thickness hold, the resin was allowed to flow, transferring a known effective stress to the fiber bed. Subsequently, the resin was allowed to gel and vitrify, and the samples were then cut, polished and inspected using a light microscope. For a fiber bed effective stress of 1 atm, the measured fiber volume fraction was Vf = 0.74. For the same effective stress, the average major and minor diameters of the elliptic tows were 2.35 mm and 0.18 mm. These values define an eccentric ellipse, which has a shorter "effective" flow length for full infiltration than the circular domain assumed in the model. To define a circular tow radius that accounts for this faster infiltration, the ellipse diameters were converted to an equivalent circular tow radius of 0.127 mm using the relation proposed by Van West et al. [26], who noted equal fill times for ellipses and circles with equal hydraulic radii:

$$R_{tow} = \sqrt{2}\frac{a_0 b_0}{\sqrt{a_0^2 + b_0^2}} \tag{6}$$

As described previously [21], the pressure boundary conditions were set in accordance with VBO processing guidelines. The resin pressure outside the porous fiber tow was assumed to be P∞ = 1.013 × 105 Pa (1 atm) due to the atmospheric consolidation pressure created by the difference between the vacuum bag and ambient atmosphere. This choice implicitly assumes that fibers and resin do not

share the applied consolidation pressure with progressive impregnation, and that no macro-flow occurs around the tows. The implications of this assumption are discussed in Section 4. The pressure at the resin flow front was assumed to be the difference between the resisting pressure of entrapped gases and the driving pressure due to capillary (wetting) action: Pf = Pgas − Pcap. The gas pressure was taken as Pgas = 0 atm, since the gas pressure in the bag was assumed to be negligible. The capillary pressure was assumed to remain constant with temperature and resin cure, and set to Pcap = 1.782 × 104 Pa (0.176 atm), as in previous work [21].

The dynamic viscosity μ was obtained from the resin property models previously developed by Kratz et al. (for the Cycom 5320 system), which predict the evolution of the degree of cure α (starting from an initial degree of cure α0) and the resin viscosity μ for any time–temperature cycle [29].

$$\frac{d\alpha}{dt} = K_1 \alpha^{m_1} (1-\alpha)^{n_1} + \frac{K_2 \alpha^{m_2} (1-\alpha)^{n_2}}{1 + e^{(D(\alpha - (\alpha_{C0} + \alpha_{CT} T)))}} \tag{7}$$

$$K_i = A_i e^{-\frac{E_{ai}}{RT}}, \quad i = 1,2 \tag{8}$$

$$\mu = \mu_1 + \mu_2 \left(\frac{\alpha_{gel}}{\alpha_{gel} - \alpha} \right)^{A + B\alpha + C\alpha^2} \tag{9}$$

$$\mu_i \cdot = A_{\mu i} e^{-\frac{E_{\mu i}}{RT}}, i = 1,2 \tag{10}$$

Eqs. (7) and (8) constitute the cure kinetics model, which serves to support Eqs. (9) and (10), the viscosity model, where t is time, T is temperature and R is the universal gas constant. In Eqs. (7) and (8), Eai is the activation energy of the resin, D is a diffusion constant, αC0 is the critical degree of

cure at absolute zero, αCT accounts for the latter's increase with temperature, and Ai, mi, and ni are constants. In Eqs. (9) and (10), Eμi is the viscosity activation energy, αgel is the degree of cure at gelation, and A, B, C and Aμi are constants. The numerical values of all constants for the resin system (Cycom 5320) are provided in Table 1 (from [24]).

Table 1: *Cure kinetics and viscosity model parameters.*

Cure kinetics model		Viscosity model	
A_1 (s^{-1})	$8.23 * 10^7$	$A_{\mu 1}$ (Pa s)	$8.0 * 10^{-13}$
E_{A1} (J/mol)	82375	$E_{\mu 1}$ (J/mol)	93931
m_1 (-)	0.75	$A_{\mu 2}$ (Pa s)	2.9 * 10-^{11}
n_1 (-)	12.46	$E_{\mu 2}$ (J/mol)	83400
A_2 (s^{-1})	$1.04 * 10^5$	α_{gel} (-)	0.48
E_{A2} (J/mol)	62355	A (-)	3.2
m_2 (-)	0.90	B (-)	12.7
n_2 (-)	2.07	C (-)	-29.6
D (-)	40.4		
α_{C0} (-)	-1.12		
α_{CT} (-) (K^{-1})	$4.53 * 10^{-3}$		

Finally, the tow permeability K was obtained by fitting the model predictions to experimental tow impregnation data measured using micro-CT in the manner described in [21]. A benchmark cure cycle was selected consisting of a 16 h room temperature vacuum hold, a 1.21 °C/min ramp to 93 °C and a hold at 93 °C. Laminates measuring approximately 100 × 150 mm, with layups of [0°/90°]2s, were partially processed to four different points within this cycle: after the 16 h room temperature hold, and after 20, 40 and 60 min of heated processing. Then, square samples measuring approximately 15 mm per side were cut from the center of each laminate and scanned using micro-CT, at the same conditions as in Section 3.1, and the X-ray micrographs obtained were used to estimate the average degree of tow impregnation β at each processing stage. The benchmark cure cycle was used as input for the tow impregnation model, and the model predictions were fit to these data points to obtain a tow permeability of $K = 6 \times 10{-}16$ m2. Note that since this value was obtained using the model, it is subject to the model assumptions and constitutes an estimate. The close fit between the predicted evolution of the tow degree of impregnation and the values measured using micro-CT is shown in Fig. 5, and a summary of the model parameters for this material is provided in Table 2.

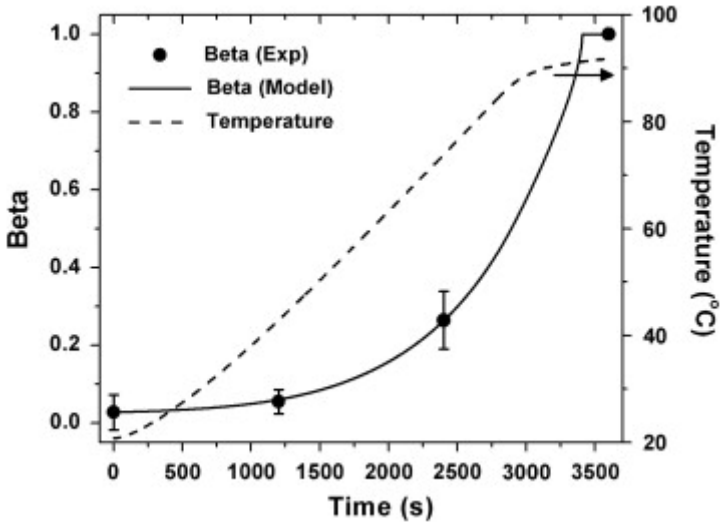

Figure 5: *Comparison of predicted and measured degrees of impregnation for the benchmark cure cycle.*

Table 2: *Summary of model parameter values*

Parameter	Value
V_f	0.74
R_{tow}	0.127 mm
P_∞	1 atm
P_f	-0.176 atm
μ	Model
K	$6 * 10^{-12}$ m^2

.

3.3. Modeling tow impregnation in aged prepregs

The effect of aging was integrated into the model by increasing the initial degree of cure α0 of the resin in the resin cure kinetics model (for 5320) and hence modifying the viscosity profile accordingly for the given time–temperature cycle. The appropriate α0 values for the out-times used to manufacture the laminates in this study were obtained in the following manner. First, for each out-time, the glass transition temperature Tg of the B-stage resin was measured using modulated differential scanning calorimetry (MDSC). For MDSC testing, a temperature ramp was performed from −90 °C to 280 °C at a ramp rate of 3 °C/min with a temperature modulation of ±1 °C every 60 s. Then, measured B-stage Tg values were input into a model linking the glass transition temperature of the 5320 resin to degree-of-cure [29], as shown in following equation:

$$\frac{T_g - T_{g0}}{T_{g\infty} - T_{g0}} = \frac{\lambda\alpha}{1-(1-\lambda)\alpha} \qquad (11)$$

In Eq. (11), Tg is the instantaneous glass transition temperature of the resin; Tg0 and Tg∞ are the glass transition temperatures for the uncured and fully cured resin, respectively, and λ is a fitting constant. As before, the numerical values of these parameters for the 5320 resin are provided elsewhere [29]. By combining the measured B-stage Tg values with Eq. (11), the initial degree-of-cure α0 associated with each prepreg age was obtained.

Finally, the tow impregnation model was used with resin viscosity profiles obtained using these α0 values, and the time–temperature cycle used to manufacture the laminates, to predict the evolution of tow impregnation and the possible occurrence of tow voids. Tow voids were quantified from the final predicted degree of impregnation β through the following geometric relation, where Av and Atow are the tow void area and the total tow area, respectively:

$$\frac{A_v}{A_{tow}} = (1-\beta)^2(1-V_f) \tag{12}$$

Table 3 shows the measured glass transition temperatures and the degrees-of-cure obtained from the model shown as Eq. (11), for the corresponding aging levels considered in this study. Results show that, as expected for B-staged prepreg resin, the initial degree-of-cure is slightly greater than zero, and both Tg and degree of cure increase with room-temperature out-time.

Table 3: *Glass transition temperatures and degrees-of-cure as a function of out-time.*

Out-time (days)	Glass transition temperature (°C)	Degree of cure × 100 (%)
0	-0.20	5.50
7	8.90	11.40
14	14.35	14.80
21	17.43	16.80
28	23.06	20.20
35	31.79	25.20
42	42.34	31.20
49	42.25	31.20
56	46.15	33.20

The increases in initial degree-of-cure α 0 due to resin aging are shown by the viscosity model to produce an increase in resin viscosity. Representative predicted viscosity profiles during the time–temperature cure cycle investigated here are shown in Fig. 6 for prepreg aged 0 days (fresh) and 56

days. The data demonstrate that during room temperature aging, the viscosity of the resin increases due to an increase in degree-of-cure of the material. Between 0 and 56 days, this increase is of at least an order of magnitude throughout the cycle. Additionally, the minimum viscosity obtained during the cure cycle is increased from roughly 101 Pa s for fresh material to ~103 Pa s after 56 days of aging.

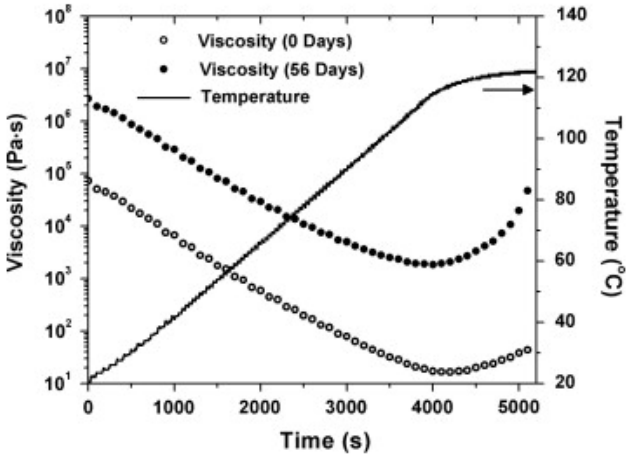

Figure 6: *Predicted influence of out-time on resin viscosity.*

The increase in resin viscosity during aging directly influences tow impregnation and void formation. Fig. 7 shows the predicted evolution of the degree of impregnation (β), as obtained through Eq. (5), as a function of cure time and temperature for fresh prepreg and pregreg aged 56 days. The fresh material reaches full tow impregnation prior to the first temperature dwell at 121 °C. In contrast, the material with an out-time of 56 days, never reaches full impregnation. In that case, the resin viscosity is already increasing rapidly by the time the 121 °C dwell is reached, preventing flow into the tows altogether.

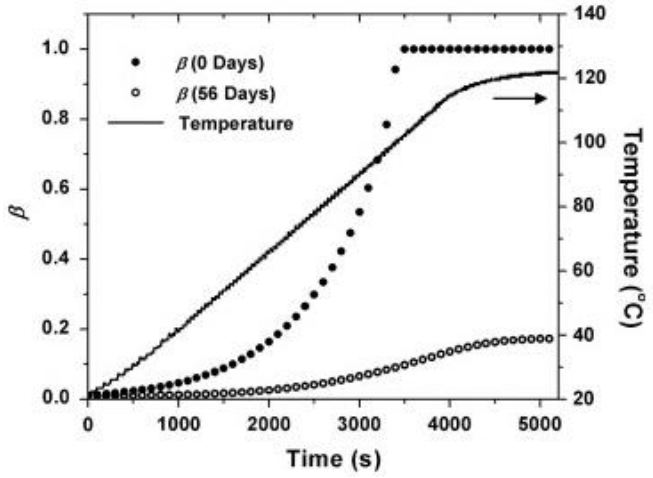

Figure 7: *Influence of out-time on the evolution of tow impregnation (β).*

Similar simulations were performed for all age times under investigation, and the final tow void content was obtained in each case. These tow void predictions are shown in Fig. 8, along with the previously described experimental values. Results indicate that within the useful out-life of the material, tow impregnation occurs fully and no tow voids are formed. Once the stated out-life is exceeded, however, tow porosity is observed. A more thorough discussion of these model predictions and the experimental data is offered in the following section.

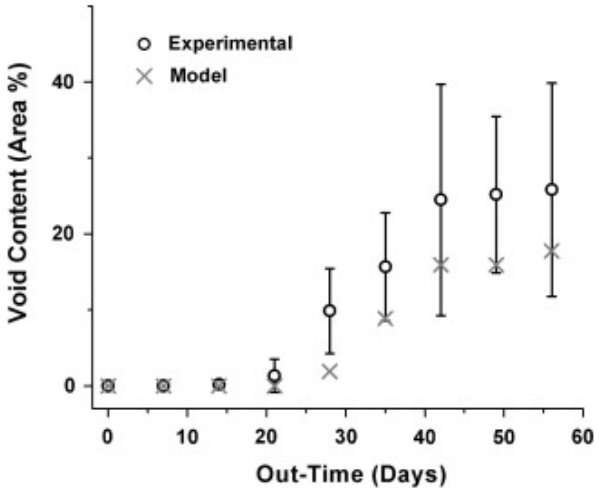

Figure 8: *Comparison of experimental and model data for void contents in laminates from aged prepregs.*

4. Discussion

One objective of this work was to develop an analytical method for predicting part quality as a function of material aging time. Fig. 8 shows that the analytical model presented here correctly predicts the onset of tow voids with increasing out-time, as well as the general trend in void content observed in the manufactured laminates. Note also that the results under-predict the average tow void content (by approximately 8–10%) at longer out-times. This discrepancy may arise from one or more of the model approximations. The model assumes perfect vacuum and neglects the influence of environmental effects, most notably, the fact that epoxy prepregs exposed to ambient conditions will absorb moisture from the air [9] and [19]. Moisture absorption can increase resin viscosity, accelerate material aging, and increase void contents [14], [15], [17], [19] and [30].

In previous work, the influence of resin moisture content on void formation in VBO processed parts was described [9]. The investigation showed that the weight percent moisture in a carbon fiber epoxy prepreg exposed to ambient humidity of 50% for 24 h increased by 25% over prepreg in the as-received condition [9]. Though a different material system was used in this work, we can assume that similar moisture absorption occurred, leading to void contents larger than expected in prepreg material stored in a dry environment.

We expect prepregs aged under desiccant to contain a smaller percentage of voids, and to correlate more closely with analytical predictions. For the model predictions, we assume that the resin pressure remains equal to 1.013 × 105 Pa (1 atm) throughout processing. However, with increasing impregnation, progressive load sharing may occur between solid and fluid phases. Thus, the resin

pressure may in fact decrease and consequently reduce the rate of infiltration, producing larger tow voids. Nevertheless, the similar trends and the accuracy of the predictions (in most cases within the margin of experimental error) indicate that the model properly accounts for the key phenomena occurring during cure, and furthermore that the increase in viscosity due to out-time is the dominant factor. Thus, the model may be used with confidence to predict part quality and to explain the features observed in the microstructure of the manufactured laminates.

Taken together, the trends exhibited by the measured and predicted data offer several insights into the relationship between aging, material properties, and final part quality. Both approaches indicate that within the manufacturer-stated out-life of 21 days, the laminates remain generally free of tow voids. The model results suggest that this can be attributed to the formulation of the resin and the evolution of viscosity, which remains sufficiently low prior to gelation for recommended time–temperature cycle to allow the required resin flow for full tow impregnation.

Furthermore, both approaches also indicate that when the out-life of 21 days is exceeded, the tow void content begins to increase. This increase is explained by the viscosity profiles for longer out-times, which exhibit both increased viscosity values over the cure cycle and earlier gelation. Because of these factors, the rate of resin flow into the tows decreases with out-time, impeding full tow impregnation.

Finally, both experiments and model results show that the detrimental effect of out-time on tow void content stabilizes after approximately 40 days, reaching a plateau. This effect is attributed to vitrification of the epoxy resin [15]. Vitrification of a thermosetting resin occurs once the glass transition temperature of the system exceeds the cure temperature (here, ambient temperature). The

Tg values reported here exceed ambient temperature after 28 days of aging time. After vitrification, the cure reaction within the resin occurs at a slower rate, leading to a gradual plateau in measured Tg values. This behavior, with Tg values increasing more slowly after temperature exceeds 20–30 °C, has been observed in a study using a different epoxy resin system [31]. Once the resin system has vitrified, the effect of increasing out-time on tow void formation diminishes.

5. Conclusions

In this study, we investigated the influence of out-time on tow impregnation for an out-of-autoclave carbon fiber/epoxy prepreg. Tow void contents were measured in laminates produced from prepreg aged for different periods of room temperature out-time. A model was developed by combining equations for flow through porous media, resin viscosity, and cure kinetics to predict the porosity remaining in a tow. Both approaches confirm that as out-time increases, porosity may remain in the tow if the resin cures faster than the tow can be saturated.

The results were obtained for a single fabric and resin system. However, as the physical phenomena involved are representative of common thermoset prepreg systems, the trends observed are of general applicability and interest. Furthermore, the analytical framework is flexible, and can be readily modified to predict aging behavior for a wide range of composite prepreg materials based on other thermoset resins and formulations.

As the use of composites in the aerospace industry increases, a critical need is developing for clearer understanding of allowable process windows and tools for predicting void content. Porosity limits for aerospace structures are typically set at 1–2%, and resin flow and compaction governs porosity and thus part quality. The primary factor influencing resin flow is viscosity, which changes during

ambient aging due to the increase in degree of cure. Understanding the influence of material out-time on impregnation and porosity is of particular importance for large composite components, where lay-up times are longer. The work presented here provides an improved understanding of the mechanisms of flow and compaction as a function of ambient aging time. Additionally, the analytical portion of the work demonstrates that the model is an effective tool for predicting part porosity for next-generation out-of-autoclave cured materials.

Acknowledgements: L.K. Grunenfelder and S.R. Nutt would like to acknowledge Airtech International for donation of the lay-up consumables used in this work. T. Centea and P. Hubert would like to acknowledge the support of the Natural Science and Engineering Research Council of Canada; the Consortium for Research and Innovation in Aerospace in Quebec; Bell Helicopter Textron; Bombardier Aerospace; Delastek; the National Research Council of Canada; the Center for Development of Composites in Quebec and McGill University, Concordia University and the University of British Columbia.

References:

1. Mortimer S, Smith MJ, Olk E. *Product development for out-of-autoclave (OOA) manufacture of aerospace structures*. In: SAMPE conference, 2010 May 17–20, Seatlle, WA; 2010.
2. Repecka L, Boyd J. *Vacuum-bag-only curable prepregs that produce void-free parts*. In: 47th international SAMPE symposium, 2002 May 12–16, Long Beach, CA; 2002.
3. Jackson K, Crabtree M. *Autoclave quality composites tooling from vacuum bag only processing*. In: 47th international SAMPE symposium, 2002 May 12–16 Long Beach, CA; 2002.
4. Farhang L, Fernlund G. *Void evolution and gas transport during cure in out-of-autoclave prepreg laminates*. SAMPE conference, 2011 May 23–26, Long Beach, CA; 2011.
5. Ridgard C. *Out of autoclave composite technology for aerospace, defence and space structures.* In: SAMPE conference, Baltimore, 2009 May 18–21 MD; 2009.
6. T. Centea, P. Hubert, *Measuring the impregnation of an out-of-autocalve prepreg by micro-CT*. Compos Sci Technol, **71** (2011), pp. 593–599

7. S. Thomas, C. Bongiovanni, S.R. Nutt, *In situ estimation of through-thickness resin flow using ultrasound.* Compos Sci Technol, **68** (2008), pp. 3093–3098
8. Louis BM, Hsiao K, Fernlund G. *Gas permeability measurements of out of autoclave prepreg MTM45-1/CF2426A.* In: SAMPE conference, 2010 May 17–20, Seattle, WA; 2010.
9. L.K. Grunenfelder, S.R. Nutt, *Void formation in composite prepregs – effect of dissolved moisture*
   Compos Sci Technol, **70** (2010), pp. 2304–2309
10. Thorfinnson B, Biermann TF. *Measurement and control prepreg impregnation for elimination of porosity in composite parts. Fabricating composites*; 1988 September 12–15; Philadelphia, PA; 1988.
11. Kratz J, Centea T, Hubert P. *Air permeability of out-of-autoclave honeycomb structures during processing*. In: The 26th annual technical conference of the American Society of Composites/the second joint US-Canada conference on composites, Montreal, QC, CA; 2011.
12. Lucas S, Howard S, Senger J. *Vacuum bag only processing; improving prepreg out-time and porosity for large composite structures*. In: SAMPE conference, 2010 May 17–20, Seattle, WA; 2010.
13. M. Akay, *Effects of prepreg ageing and post-cure hygothermal conditioning on the mechanical behaviour of carbon–fibre/epoxy laminates.* Compos Sci Technol, **38** (1990), pp. 359–370
14. R.W. Jones, Y. Ng, J.F. McClelland, *Monitoring ambient-temperature aging of a carbon-fiber/epoxy composite prepreg with photoacoustic spectroscopy.* Composites: Part A, **39** (2008), pp. 965–971
15. Y. Gu, M. Li, Z. Zhang, Y. Li, *Effects of resin storage aging on rheological property and consolidation of composite laminates.* Polym Compos (2009), pp. 1081–1090
16. L.K. Grunenfelder, S.R. Nutt, *Out time effects on VBO (vacuum bag only) prepreg and laminate properties.* SAMPE J, **47** (2011), pp. 6–13
17. K.C. Cole, D. Noel, J.-J. Hechler, et al., *Room temperature aging of Narmco 5208 carbon–epoxy prepreg. Part I: physicochemial characterization.* Polym Compos, **10** (1989), pp. 150–161
18. K.C. Cole, D. Noel, J.-J. Hechler, et al., *Room-temperature aging of Narmco 5208 carbon-epoxy prepreg. Part II: physical, mechanical, and nondestructive characterization.* Polym Compos, **12** (1991), pp. 203–212
19. D.A. Scola, J. Vontell, M. Felsen, *Effects of ambient aging of 5245C/graphite prepreg on composition and mechanical properties of fabricated composites.* Polym Compos, **8** (1987), pp. 244–252
20. Wysocki M, Larsson R, Toll S. *Modelling the consolidation of partial impregnated prepregs. In: ICCM-17 17th international conference on composite materials*, 2009 July 27–31 Edinburgh, UK; 2009.
21. T. Centea, P. Hubert, *Modelling the effect of material properties and process parameters on tow impregnation in out-of-autoclave prepregs*. Composites: Part A (2012)
22. S. Thomas, S.R. Nutt, *Temperature dependence of resin flow in a resin film infusion (RFI) process by ultrasound imaging.* Appl Compos Mater, **16** (2009), pp. 183–196
23. Cytec. CYCOM 5320 information sheet; 2009.

24. Centea T, Hubert P. *Experimental observations and analytical modelling of the resin flow inside an out-of-autoclave prepreg*. In: The 10th international conference on flow processes in composite materials (FPCM10), 2010 July 11–15, Monte Verita, Ascona, CH; 2010.
25. V. Neacsu, A.A. Obaid, S.G. Advani, *Spontaneous radial capillary impregnation across a bank of aligned micro-cylinders – Part I: theory and model development.* Int J Multiph Flow, **32** (2006), pp. 661–676
26. B.P. Van West, R.B. Pipes, S.G. Advani, *The consolidation of commingled thermoplastic fabrics.* Polym Compos, **12** (1991), pp. 417–427
27. M.E. Foley, J.W. Gillespie Jr., *Modeling the effect of fiber diameter and fiber bundle count on tow impregnation during liquid molding processes*. Journal of Composite Materials, **39** (2005), pp. 1045–1065
28. N. Bernet, V. Michaud, P.E. Bourban, J.-A.E. Manson, *An impregnation model for consolidation of thermoplastic composites made from commingled yarns.* J Compos Mater, **33** (1999), pp. 751–772
29. J. Kratz, K. Hsiao, F. Goran, P. Hubert, *Thermal models for MTM45-1 and Cycom 5320 out-of-autoclave prepreg resins.* J Compos Mater (2012)
30. Grunenfelder LK, Nutt SR. *Moisture and pressure effects on void formation in prepreg processed composites.* In: American Society for Composites (ASC) 25th technical conference, 2010 September 20–23, Dayton, OH; 2010.
31. M. Frigione, J.M. Kenny, *Thermokinetic effects of the aging of epoxy matrix prepregs for high performance composites.* Polym Compos, **23** (2002), pp. 530–537